

Original

Metakaolin and demolition wastes in eco-based sand consolidated concrete



Khalil Lazaar^{a,b,*}, Walid Hajjaji^c, Bechir Moussi^a, Fernando Rocha^d, Jao Labrincha^e, Fakher Jamoussi^a

^a Georessources Laboratory, CERTE, 273 – 8020 Soliman, Tunisia

^b University of Gabes, Faculty of Sciences of Gabes, 6072 Zrig, Tunisia

^c Natural Water Treatment Laboratory, CERTE, 273 – 8020 Soliman, Tunisia

^d Geobiotec, Geosciences Department, University of Aveiro, 3810-193 Aveiro, Portugal

^e Department of Materials and Ceramic Engineering/CICECO – Aveiro Institute of Materials, University of Aveiro, 3810-193 Aveiro, Portugal

ARTICLE INFO

Article history:

Received 4 November 2019

Accepted 26 February 2020

Available online 21 April 2020

Keywords:

Silica sand

Metakaolin

Demolition materials

Geopolymers

Mechanical properties

ABSTRACT

This study was undertaken to valorize naturally occurring silica sand in the synthesis of new consolidated concrete materials. The mixtures of silica sand, calcium sulphate, commercial metakaolin, demolition materials were designed to propose sulphate and sodium silicate/NaOH activate concretes and geopolymers, respectively. Three raw silica sand samples were collected from various locations in Tunisia. The obtained new materials were characterized by SEM and mechanical properties were investigated.

The calcium sulphate-based concretes displayed good technological properties with a compressive strength close to 15 MPa and 40–56% of water adsorption. When, metakaolin and demolition reject were added the mechanical resistance decreased due to the lower pozzolanic properties of these materials.

Concerning the geopolymer-based sand concrete, lower compressive strength values were registered. Moreover, by incorporating demolition materials, the mechanical resistance decreased in all consolidated products. The effect of the metakaolin reactivity is more significant when it is activated with an alkaline solution. However, the sodium silicate/NaOH activation of metakaolin governs the reaction when it is highly reactive.

Finally raw silica sand from Tunisia provided good consolidated concrete materials in the presence of calcium sulphate. As well, the silica sand provided good geopolymers in the presence of metakaolin and alkaline solution.

Published by Elsevier España, S.L.U. on behalf of SECV. This is an open access article under the CC BY-NC-ND license (<http://creativecommons.org/licenses/by-nc-nd/4.0/>).

* Corresponding author.

E-mail address: lazaar.khalil@yahoo.fr (K. Lazaar).

<https://doi.org/10.1016/j.bsecv.2020.02.004>

0366-3175/Published by Elsevier España, S.L.U. on behalf of SECV. This is an open access article under the CC BY-NC-ND license (<http://creativecommons.org/licenses/by-nc-nd/4.0/>).

Desechos de metacaolín y demolición en concreto consolidado con arena con base ecológica

R E S U M E N

Palabras clave:

Arena de sílice
Metacaolín
Materiales de demolición
Geopolímeros
Propiedades mecánicas

Este estudio se realizó para valorizar la arena de sílice natural en la síntesis de nuevos materiales de hormigón consolidado. Las mezclas de arena de sílice, sulfato de calcio y metacaolín comercial, materiales de demolición se diseñaron para proponer sulfatos y silicatos de sodio/NaOH activan concretos y geopolímeros, respectivamente. Se recogieron tres muestras de arena de sílice en bruto de varios lugares en Túnez. Los nuevos materiales obtenidos se caracterizaron por SEM y se investigaron las propiedades mecánicas.

Los hormigones a base de sulfato de calcio mostraron buenas propiedades tecnológicas, con una resistencia a la compresión cercana a 15 MPa y con el 40-56% de adsorción de agua. Cuando se agregaron metacaolín y rechazo de demolición, la resistencia mecánica disminuyó debido a las propiedades puzolánicas más bajas de estos materiales.

Con respecto al hormigón de arena a base de geopolímero, se registraron valores de resistencia a la compresión más bajos. Además, al incorporar materiales de demolición, la resistencia mecánica disminuyó en todos los productos consolidados. El efecto de la reactividad del metacaolín es más significativo cuando se activa con una solución alcalina. Sin embargo, la activación de silicato de sodio/NaOH del metacaolín gobierna la reacción cuando es altamente reactivo.

Finalmente, la arena de sílice cruda de Túnez proporcionó buenos materiales de hormigón consolidado en presencia de sulfato de calcio. Además, la arena de sílice proporcionó buenos geopolímeros en presencia de metacaolín y solución alcalina.

Publicado por Elsevier España, S.L.U. en nombre de SECV. Este es un artículo Open Access bajo la licencia CC BY-NC-ND (<http://creativecommons.org/licenses/by-nc-nd/4.0/>).

Introduction

The development of new building materials is a topical issue where researchers are trying to find suitable low-cost materials. The upgrading of silica sands in the manufacture of silica-based bricks concretes and the reuse of construction waste materials with metakaolin and calcium sulphate as additions to bricks can help to overcome the noticed huge deficit in building materials. In addition, the use of locally available natural materials facilitates the manufacture of bricks and reduces the cost of construction. The bricks based on silica sands has the advantage of responding to climatic constraints (insulation). These natural silica sand could be potentially used as raw materials for the synthesis of a novel class of materials; silica bricks (consolidated concrete).

With an average of one tonne per year per habitant of cement produced each year for every human in the world, the cement industry is logically the second major producer of the greenhouse gas in our planet [1]. Hence, diminishing CO₂ emission could be obtained by reducing the use OPC in producing concrete. The development of new building eco-materials is current issues where researchers are trying to find suitable low cost and environmentally friendly products.

Calcium sulphate show great promise in this respect, having been shown to embody emissions reductions of as much as 49% [2,3] compared to traditional OPC (Ordinary Portland Cement). Calcium sulphate appears to be a potential alternative because of excellent mechanical performance, high mechanical strength at early ages, rapid-hardening, high impermeability, and chemical resistance [4,5].

Presented as third generation of cement after calcium sulphate and OPC, metakaolin based geopolymers concretes are considered as a first-class substitute cement. It is valued that, depending of the precursors and activators, the production of geopolymers results around 70% less greenhouse gas emissions than the production of cement, which makes some geopolymers environmentally friendly [6,7]. Metakaolin remains the ideal and commonly used precursor because of its high purity and reactivity [8,9]. Due to its reactivity, this calcined clayey material can generate the formation of consolidated network. Recent investigations are focusing in optimizing technological properties of geopolymer based concretes such as high resistance at early ages, resistance to chemical attack, low thermal and acoustic conductivity, and high temperature. These properties are depending in the activators (NaOH, ratio of Si/Al, Na or K-based activator) [1] and more important the used binder (sand [1,10]).

The upgrading of natural available sands in the manufacture of silica-based concrete with low CO₂ emission process [11]. Obviously, the use of such materials has the benefit of replying to climatic constraints (insulation), low manufacturing energy consumption and low CO₂ emission [12]. Furthermore, recent studies determined that improvements in reducing greenhouse emissions using such sand based consolidated concretes could reach 44–64% [13]. In addition, the use of local available natural materials is very decisive in the final market price and the compactivity of this building material.

In Tunisia, these raw materials have a significant economic value and are an integrated part of the supply chain of several industries. The annual global production of silica sand

was approximately 140 Mt/year [14]: USA (24%), Netherlands (20%), and France (5%) in 2011. Silica sand is primary ingredient material several industries; in all glass industry, in foundries to make moulds, ceramics, electronic devices, . . . More important to this study, the silica sand are material resources for silica brick, consolidated concrete manufacturing and other building materials. It is relevant to evoke that Tunisia imports huge amounts of silica sand (from countries like Spain, Germany, Belgium, USA, Italy, Mexico and France) with big draw backs in its economy trade balance.

Moreover, demolition waste materials could also be an interesting binder alternative. This material causes a critical environmental problem because of its durability and the absence of its degradation [15]. Now, using the demolition materials as a source of aggregates to make a new concrete becomes very interesting for the construction industry [16]. In fact, recycled construction materials are more porous, with a higher water absorption, hydrates content, and have good pozzolanic properties [17].

We should say that the selected process is eco-friendly, since it involves low energy and common raw materials . . . while is adaptable for accepting the sand, the raw material targeted for valorization.

This work aimed to promote local georesources (silica sand) for the preparation of consolidated concrete. With this raw material, hydraulic binders were added to the production of consolidated concrete, such as calcium sulphate (H) metakaolin (MK) and construction demolition materials (W).

Silica sand is primary ingredient material for silica brick manufacturing. Demolition waste materials are interesting due to its high porosity. Calcium sulphate matrix is interesting from an environmental point of view since it requires low embodied energy and generates low CO₂ emissions. The

expected thermal insulation properties make it suitable for interior partitions of buildings, while is easy to mould/work.

Experimental details

Geological settings

In this study, three different sand samples were collected from the Fortuna formation and Sidi Aich formation deposits. The deposits of the Fortuna from Menchar (M) are located about 15 km south of Hammamet. These quartz sands appear in the channels interspersed with clayey materials, silt and rarely consolidated sandstone [18,19]. The Sidi Aich formation presents white fine silica sands with rare clays and carbonates intercalations constituents. The Sidi Aich formation occurs as continuous outcrops, between the central and southwestern parts of Tunisia [18,20–24]. These sands were collected in the localities of Jebel Attaf (A) and Jebel Sidi Aich (SA).

Bricks synthesis procedure

Calcium sulphate matrix

Hardened concretes were tested by adding silica sands treated (J. Menchar (M), J. Sidi Aich (SA) and J. Attaf (A)), metakaolin 1200S (MK) (AGS Minerals, France) as source of aluminosilicate and calcium sulphate (H) and construction demolition materials (W). After that mixing of materials in a shaft mixer for 2 min, 5 g of water was added and the mixture was homogenized for further 2 min. The different compositions were subjected to a pressure of 2 bars (Fig. 1a). The hardened concretes were manufactured in a cylindrical mould of

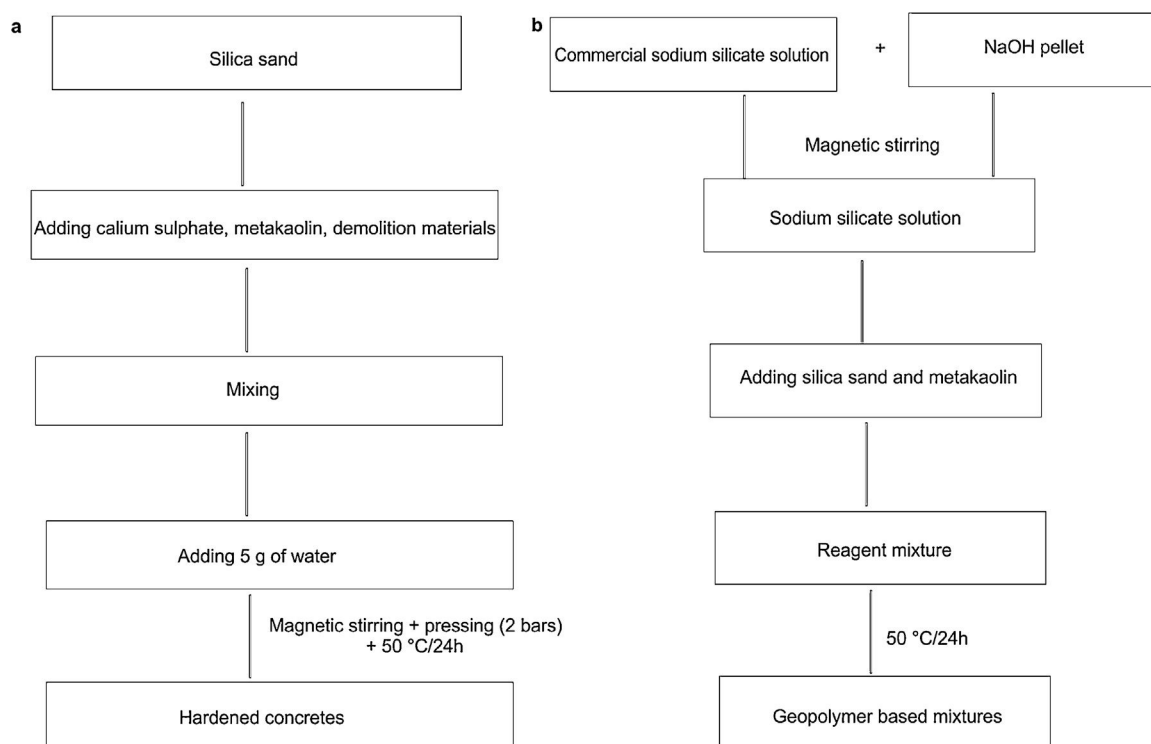
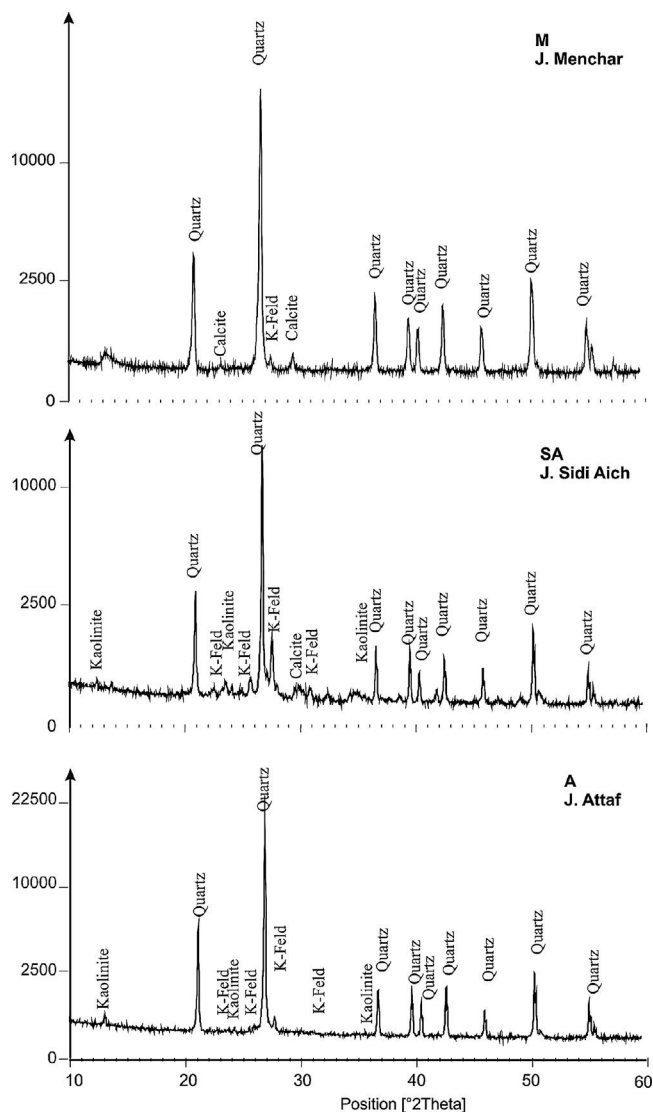


Fig. 1 – Protocol of hardened concretes synthesis (a) and protocol of geopolymer based mixtures synthesis (b).

Table 1 – Mixtures (in %) of manufactured concrete matrix.

	Sand (S)	Metakaolin (MK)	Calcium sulphate (H)	Demolition materials (W)	NaOH	Sodium silicate	Pressing (bar)
<i>Calcium sulphate based mixtures</i>							
SHMK	40	5	5	–	–	–	2
SHW	40	–	5	5	–	–	2
SH	40	–	10	–	–	–	2
SMK	40	10	–	–	–	–	2
<i>Geopolymer based mixtures</i>							
SMKG	40	10	–	–	4	6	–
SWG	40	–	–	10	4	6	–
A25	25	25	–	–	6	15	–
A50	50	25	–	–	6	15	–
A75	75	25	–	–	6	15	–
A85	85	25	–	–	6	15	–

**Fig. 2 – XRD patterns of the collected silica sand samples.**

3 cm diameter and 4.5 heights with different compositions (sand, calcium sulphate, metakaolin and demolition materials). Table 1 shows the concrete products containing different compositions.

Mineralogical analysis of samples and final materials (hardened concretes and geopolymers) were carried out by X-ray diffraction (XRD) using “X’PERT PRO Philips Analytical” diffractometer using monochromated Cu K α radiation in the 10–80° 2 θ range, scan rate of 0.02° (2 θ), and 185 s equivalent per step [25]. The composition of the chemical major elements of materials was obtained from the chemical analysis determined by X-ray fluorescence using Philips X’UNIQUE apparatus [25]. The particle size distribution was carried by a laser Coulter LS230. FT-IR spectrum of hardened concretes and geopolymers was carried out using a PerkinElmer model spectrometer. The compressive strength was tested using a Shimadzu (Model: AG-X/R Refresh) universal testing machine with a crosshead speed of 0.5 mm/min according to the Standard EN 1015-11. The value is calculated from the following equation (Eq. (1)):

$$CS = \frac{F}{S} \quad (1)$$

where CS (MPa) is the compressive strength, F (KN) is the force of breaking specimens and S (cm²) is the surface area of specimens.

We determined the water absorption, the open porosity and bulk density according to ASTM: C373 on 3 fragments after mechanical test. The fragments were dried at 105 °C and then weighed, it records the dry mass m_s and then put the pieces in water at 120 °C for 3 h and then record the wet mass m_h [26,27]. The value is calculated from the following equation (Eq. (2)):

$$W (\%) = \left(\frac{m_h - m_s}{m_s} \right) \times 100 \quad (2)$$

where W (%) is the adsorption of water expressed as percentage; W_h (g) is the mass after absorption test and W_s (g) is the dry mass of the sample [28].

The microstructural details of the final products were observed using a Hitachi SU 70 scanning electron microscope (SEM).

Sodium silicate matrix (geopolymer based mixtures)

The second variety of consolidated concrete was confectioned using the same materials; silica sands (S) with metakaolin (MK) (was used as a precursor of aluminium), construction demolition materials (W) and alkaline solutions. In water medium, alkaline activators NaOH (ACS AR Analytical Reagent

Table 2 – X-ray fluorescence analysis of the collected sands samples and hydraulic binder.

Oxides	M	SA	A	MK	W	H
SiO ₂	98	85	97	54	59	0.6
Al ₂ O ₃	1.1	7	1.1	39.5	7	0.2
K ₂ O	0.2	5.6	0.5	1	1.1	0.1
Fe ₂ O ₃	0.3	0.5	0.4	1.8	3.9	0.1
MnO	–	–	–	–	0.1	–
MgO	–	–	–	0.1	1.4	0.6
CaO	0.1	–	–	0.1	18	41.8
TiO ₂	0.1	0.6	0.6	1.6	0.4	–
Cr ₂ O ₃	0.1	–	–	–	–	–
SO ₃	–	–	–	–	1.3	54
Na ₂ O	–	–	–	–	0.4	–
P ₂ O ₅	–	–	–	–	0.1	–
LOI	0.5	0.9	0.3	2.7	7	2.6

Grade Pellets) and hydrated sodium silicate (Merck, Germany; 8.5 wt.% Na₂O, 28.5 wt.% SiO₂, 63 wt.% H₂O) were used to dissolve aluminosilicate and avoid residual sodium [25]. These materials were added and thoroughly mixed.

The mixing of the blends was carried out by Heidolph ST-1 Laboratory stirrer at 100rpm for 2 min, to ensure their homogeneity and avoid bubbles and agglomeration into the sample (Fig. 1b). The pastes were immediately poured into 30 mm × 45 mm cylindrical moulds and placed in oven at 50 °C for 24 h. Curing silica bricks cylindrical specimens was carried from 1, 7, 14, 21 and 28 days.

Results

Raw materials characterization

Silica sand

Fig. 2 shows the mineralogical analysis of the silica sand used in preparation of consolidated concrete. The XRD patterns of studied sands revealed the predominance of quartz (90–98%) and potassic feldspars (1–9%) as the main constituents. Minor proportions of kaolinite (0–1%) and calcite (0–1%) were also detected. The dominance of quartz suggests that the depositional basins were associated with a passive margin [29]. The presence of potassic feldspars shows that the source of these silica sands could be probably of magmatic origin or even metamorphic from the Hoggar Massif [30]. The chemical composition (Table 2) used sands showed relatively low contents in Al₂O₃, K₂O, Fe₂O₃ and TiO₂. The two first oxides are associated to the presence of potassic feldspars, when the rest are coupled to non-depicted heavy metals [22]. By laser interference we quantified the particle sizes of the finer fraction as 100.6 μm, 127.2 μm and 108.5 μm, respectively, for samples of M, A and SA (Fig. 3).

Calcium sulphate, metakaolin and demolition materials

The XRD patterns of studied calcium sulphate (H) and metakaolin (MK) are reported in Fig. 4. The studied calcium sulphate (H) shows a broad reflection centred $2\theta = 27^\circ$ attributable to the bassanite with the presence of dolomite. This material is prepared from the mineral, gypsum. These can set hard and be used for various purposes, e.g., for dam building materials in mines and as plaster for medical

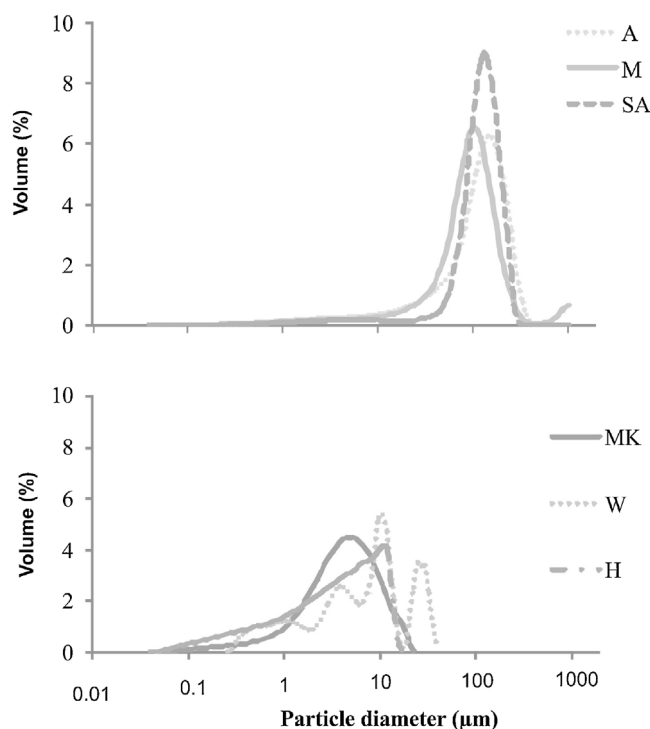


Fig. 3 – Particle size distribution of used materials. A: silica sand of J. Attaf; M: silica sand of J. Menchar; SA: silica sand of J. Sidi Aich; H: calcium sulphate; MK: metakaolin and W: demolition materials.

and dental purposes. The metakaolin (MK) shows a broad reflection centred at $2\theta = 24^\circ$ attributable to the amorphous materials. The peaks of quartz and illite are clearly visible. Also traces of anatase are detected. These results for XRD powder patterns of the metakaolin are close to those reported by [25] who studied the composition and technological properties of geopolymers based on metakaolin and red mud. The XRD powder patterns of studied demolition materials (W) show the predominance of quartz and calcite.

The composition of the chemical major elements is reported in Table 2. The calcium sulphate (H) is predominantly composed by sulphur trioxide (54%) and calcium oxide (41.8%). Metakaolin (MK), used in this study, showed relatively high silicon dioxide content (54%). The mass ratio SiO₂/Al₂O₃

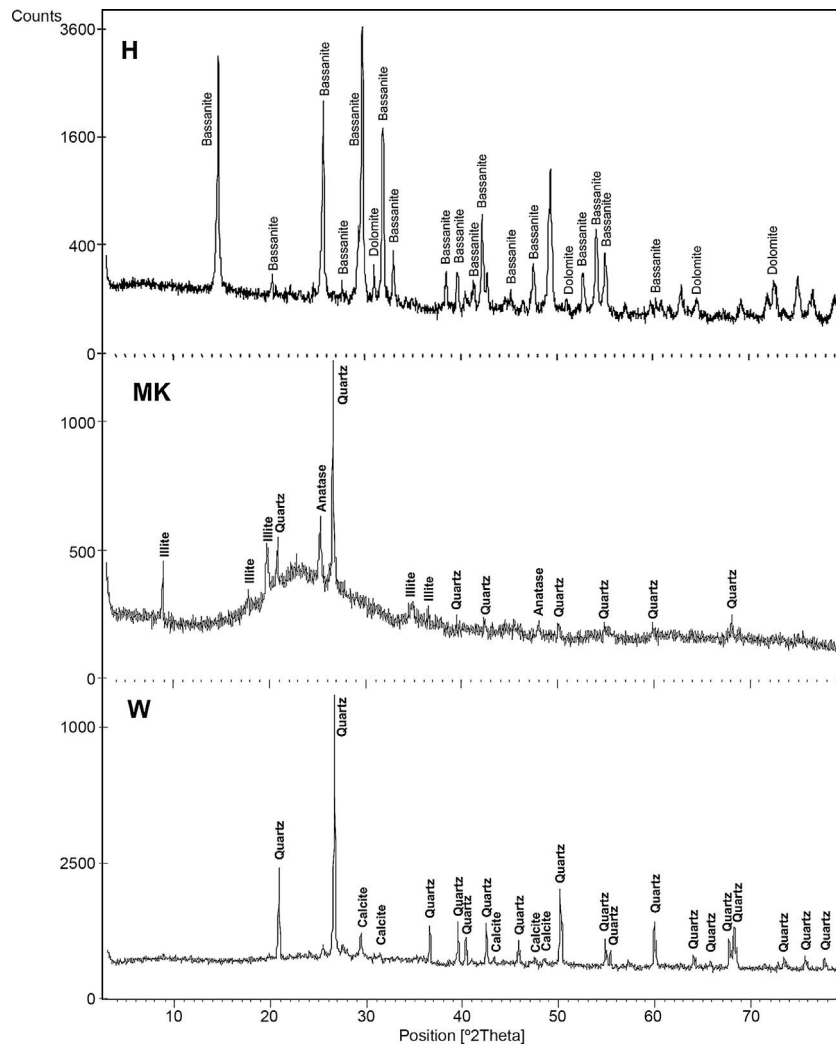


Fig. 4 – XRD patterns of calcium sulphate (H), metakaolin (MK) and demolition materials (W).

equals 1.38 which is much higher than pure metakaolin (mass ratio $\text{SiO}_2/\text{Al}_2\text{O}_3 = 1.2$) due to presence of quartz. Concerning the construction demolition materials (W), the chemical composition is mainly of silicon dioxide (59%) and calcium oxide (18%).

The particle size distribution of (MK) is coarser (mean size around $4.44\ \mu\text{m}$) than that of (H) one (mean size is below to $3.9\ \mu\text{m}$) (Fig. 3). This may suggest the presence of higher amounts of impurities (quartz and anatase) in the metakaolin that can cause the particle size distribution to increase [31]. The particle size distribution of W is coarser (mean size around $250\ \mu\text{m}$) than that of MK and H.

Consolidated concrete properties

X-ray diffraction (XRD) analysis of hardened concretes and geopolymer

XRD (X-ray diffraction) patterns of hardened concretes (SHMK-M, SHW-M) and geopolymers based mixtures (SMKG-M, SWG-M) are reported in Fig. 5. The XRD of the final material SHMK shows the presence of quartz associated to illite and bassanite. The XRD of hardened concretes SHW shows

the presence of quartz associated to calcite. The patterns of geopolymer based mixtures (SMKG-M) show a slightly broad reflection related to the amorphous content, like that observed for metakaolin. Nevertheless, the centre of this reflection is shifted to $2\theta = 31^\circ$ due to changes in composition and structure when metakaolin is activated by NaOH and NaSiO_2 solutions. Moreover, diffractions of metakaolin admixtures as illite and quartz, which stayed unreacted, are still present in SMKG-M. Which implies that geopolymerization reactions is not very evident (may be related to insufficient quantity of metakaolin).

FT-IR spectrum analysis

The FTIR spectra were collected to obtain a better insight into the surface characteristics of the final materials (Fig. 6). The bands at $1060\ \text{cm}^{-1}$ and $1090\ \text{cm}^{-1}$ are related to Si–O–Si stretching vibrations of the surface and bulk of unreacted silica particles respectively.

The main bands at $952\ \text{cm}^{-1}$, $945\ \text{cm}^{-1}$ and $975\ \text{cm}^{-1}$ are related to the presence of newly formed geopolymer gel regions with different Si/Al ratios in their gel networks. The band at $850\ \text{cm}^{-1}$ is related to the vibration of Si–OH bonds, and the existence of a significant peak at this wavenumber

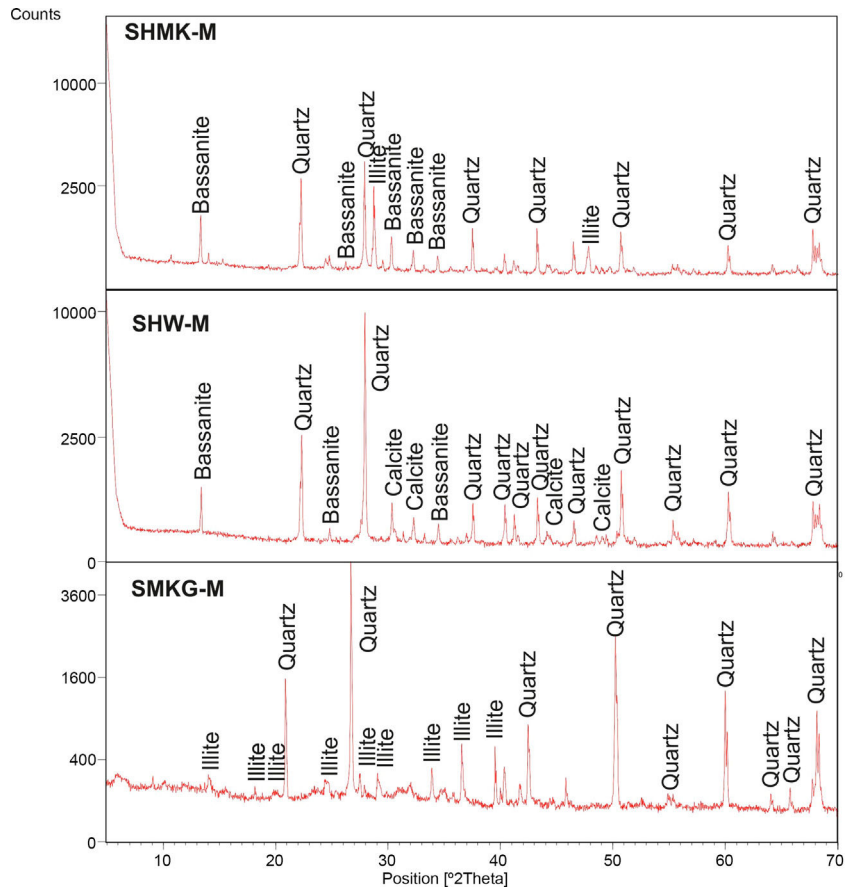


Fig. 5 – XRD patterns of consolidated concretes (SHMK-M, SHW-M) and geopolymer (SMKG-M). S: sand; H: calcium sulphate; MK: metakaolin; W: demolition waste; G: NaOH and NaSiO₂ solutions; -M: Menchar.

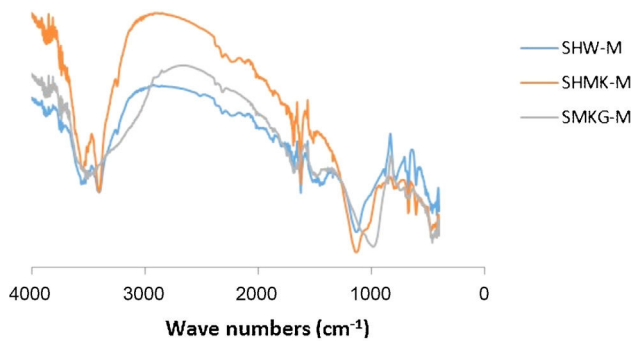


Fig. 6 – FT-IR spectra of the hardened concretes and geopolymers. S: sand; H: calcium sulphate; W: demolition waste; MK: metakaolin; G: NaOH and NaSiO₂ solutions; -M: Menchar.

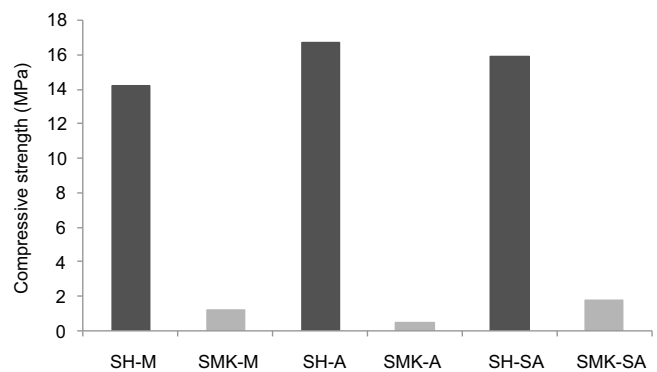


Fig. 7 – Comparison between calcium sulphate (H) and metakaolin (MK) based concretes (-M: Menchar; -A: Attaf and -SA: Sidi Aich).

for some regions in SMKG-M sample indicates the presence of silica species which have not yet fully participated in geopolymerization after of curing. The following characteristic infrared signals were observed: Si-O bending (469 cm^{-1}) and Si-O (689 cm^{-1}). The bands at 524 and 734 cm^{-1} , corresponding to “pore opening” vibration and to symmetric stretching of free SiO₄, also appeared. Fig. 6 also shows an OH group vibration zone between 3700 and 3400 cm^{-1} for the valence bands.

Compressive strength

The results of compressive strength of calcium sulphate-based concretes are reported in Figs. 7 and 8. The compressive strength gave maximum values of the consolidated concrete prepared from the silica sand M, A, SA with a small amount of calcium sulphate (H) (14.2 MPa , 16.7 MPa and 15.9 MPa for SH-M, SH-A, SH-SA respectively). By introducing metakaolin (MK) instead of calcium sulphate (W) and with J. Menchar (M),

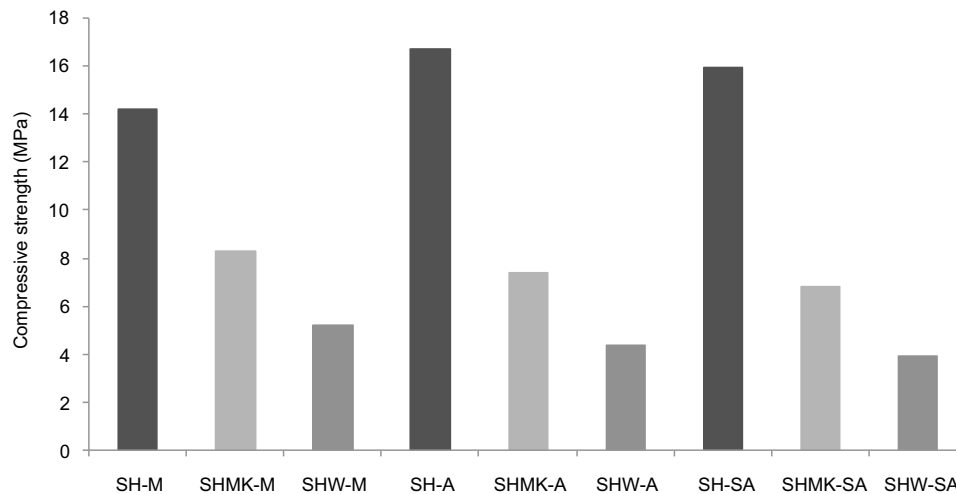


Fig. 8 – Compressive strength of hardened concrete; influence of addition of calcium sulphate (H); metakaolin (MK) and demolition wastes (W) (-M: Menchar; -A: Attaf and -SA: Sidi Aich).

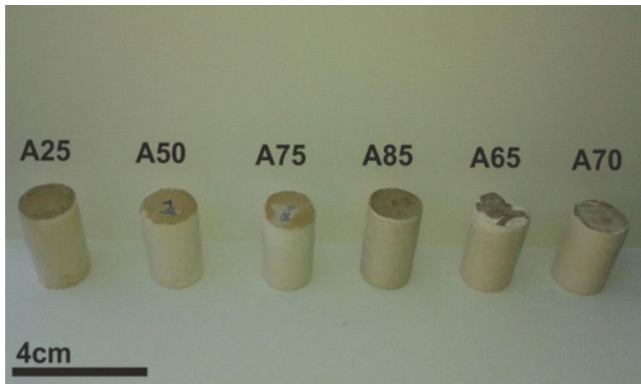


Fig. 9 – Consolidated concrete made with geopolymeric matrix.

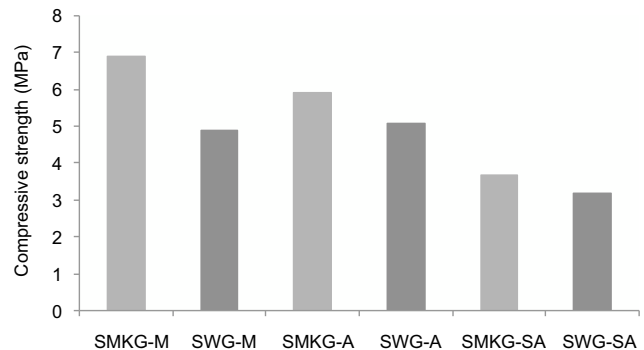


Fig. 10 – Influence of substitution of metakaolin (MK) by demolition wastes (W) in compressive strength of geopolymeric-based concrete. (-M: Menchar; -A: Attaf and -SA: Sidi Aich).

J. Sidi Aich (SA) and J. Attaf (A) sands, the compressive strength is decreased (less than 2 MPa) (Fig. 4).

By adding a small amount of either metakaolin or construction demolition materials to the calcium sulphate, the compressive strength of the consolidated concrete decreased compared to those made from calcium sulphate (Fig. 8). This may be due to the large size of the demolition particles.

Other types of specimens were made from silica sands, metakaolin (MK), construction demolition materials (W) and geopolymer matrix (G) (NaOH and sodium silicate). Fig. 9 shows the consolidated concrete containing variable amounts of metakaolin, demolition materials with geopolymer matrix. With the introduction of the geopolymer based matrix, a clear improvement in the mechanical properties of concrete samples prepared from silica sand and metakaolin was observed (Fig. 10).

Replacing metakaolin (MK) by demolition materials (W), the compressive strength decreased by approximately 25% in all consolidated (Fig. 10). This behaviour should be connected to the binder particle size and Si/Al matrix ratio.

The observed microstructures (Fig. 11) are characteristic of a consolidation material with fine grain and amorphous matrix [32].

Water absorption test

The results of water absorption are reported in Fig. 12. Concerning the first type of consolidated concretes, it is observed that the products obtained from simple compaction with calcium sulphate or metakaolin absorbs almost half weight in water (40–56%).

The water absorption of the calcium sulphate hardened concretes registered an increase by addition of metakaolin and more with incorporation of demolition materials due to the higher particle size of these merged materials (reaching 58% for SHW-SA) (Fig. 13).

With the incorporation of the geopolymer-based matrix, water absorption results for the sand, metakaolin and demolition materials products ranged between 21 and 25% (Fig. 14). In function of curing period, it is noticeable that water absorption values are practically unchangeable from 1 until 28 days

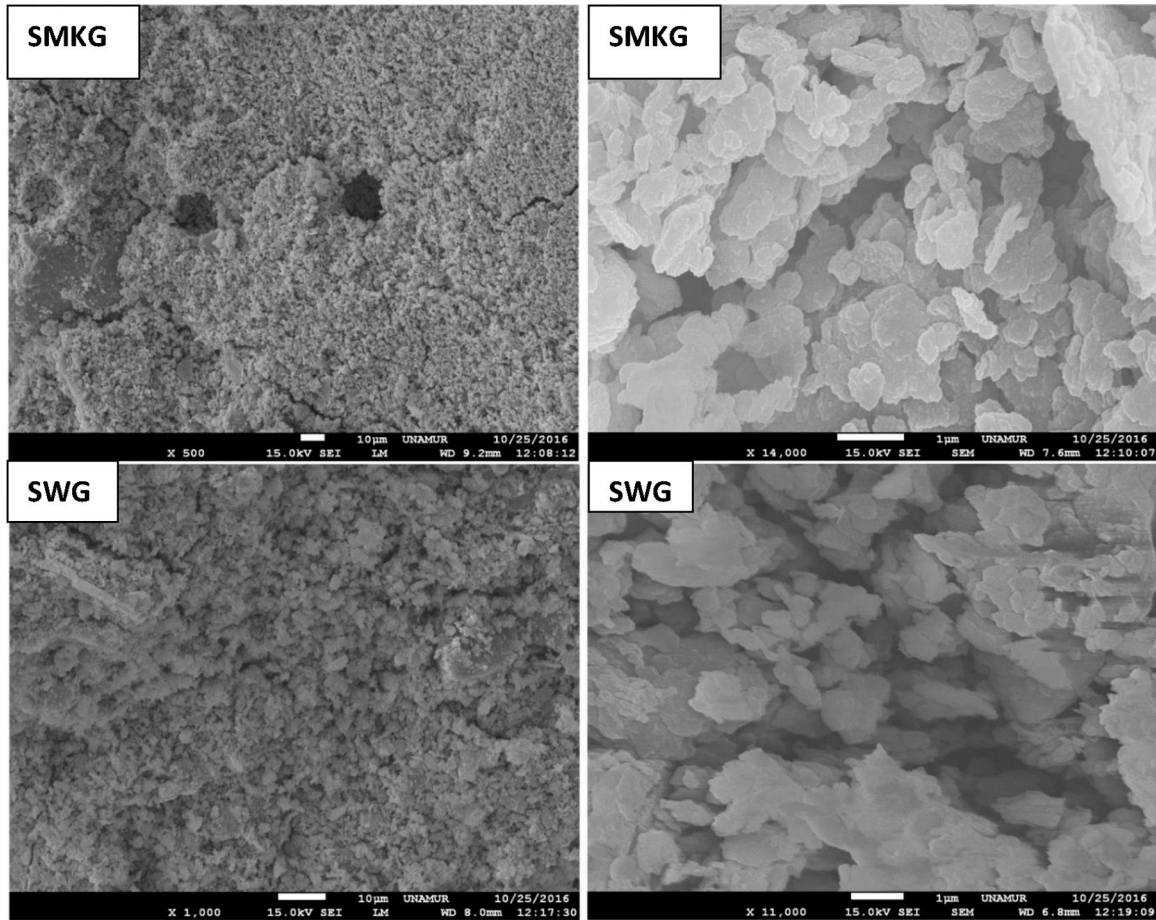


Fig. 11 – SEM micrographs of consolidated concrete.

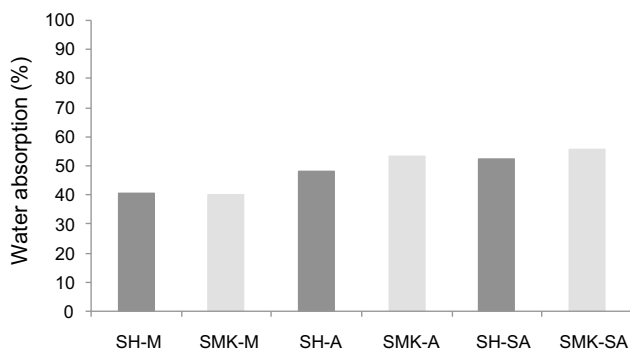


Fig. 12 – Water absorption of hardened concretes. (-M: Menchar; -A: Attaf and -SA: Sidi Aich).

for geopolymer consolidated concrete M85 (ratio 85:15; around 29%) (Fig. 15). The same value was measured in SA85 sample, when in A85 the water absorption decreased (Fig. 16).

Table 3 shows the water absorption, open porosity and bulk density of a some consolidated concretes and geopolymers cured. The consolidated concretes (SHM-M, SHW-M) present similar behaviour with high values of water absorption (51–56%) and open porosity, while low bulk density (1.02–1.05 g/cm³). On the other hand, geopolymers (SMKG-M,

SWG-M) present lower water absorption values (51–56%) and open porosity than those obtained by consolidated concretes, while an apparent density slightly higher than that of consolidated concretes (1.11–1.12 g/cm³).

Discussions

Unlike calcium sulphate, metakaolin shows no strong properties in the hydraulic binder. In contact with water, calcium sulphate forms a rigid and relatively strong lattice. The respective exothermic reaction is fast.

Using the alkaline solutions the products SMKG-M, SMKG-SA and SKG-A, the compressive strength reached almost 7 MPa with increasing a content of 5% of metakaolin (less than 2 MPa without a geopolymer matrix).

The presence of quartz and metakaolin (Fig. 11) observed as partially reacted vestiges suggests that the silica provided by sodium silicate is more active in the geopolymerization process than the silica introduced by metakaolin [25,33]. Traces of unreacted MK (Fig. 11) simply means that reactivity was not complete: formulation was not optimized or curing conditions were not the most favourable.

From Fig. 17 it is obvious that compressive strength values show an increasing trend from 1 until 28 days for geopolymer consolidated concrete M85 (from 2.5 MPa to 3.3 MPa).

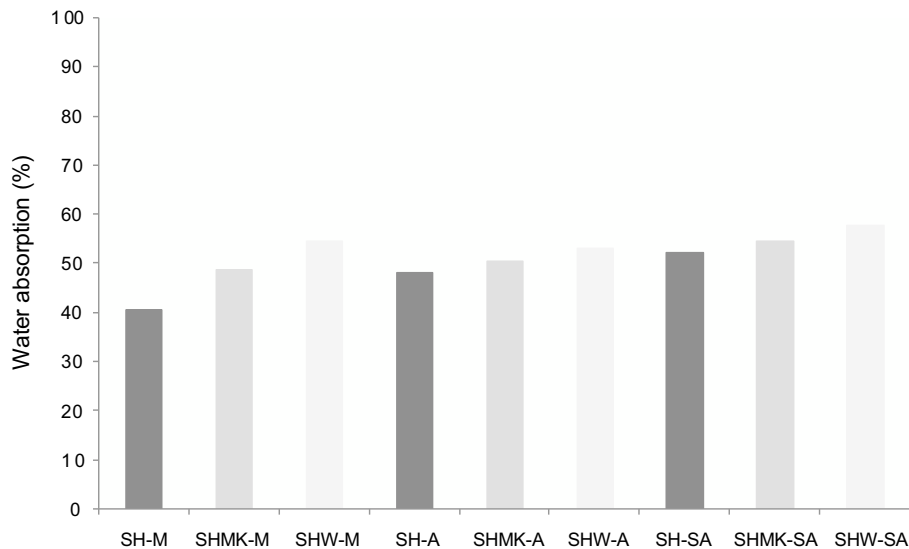


Fig. 13 – Water absorption of hardened concretes. (-M: Menchar; -A: Attaf and -SA: Sidi Aich).

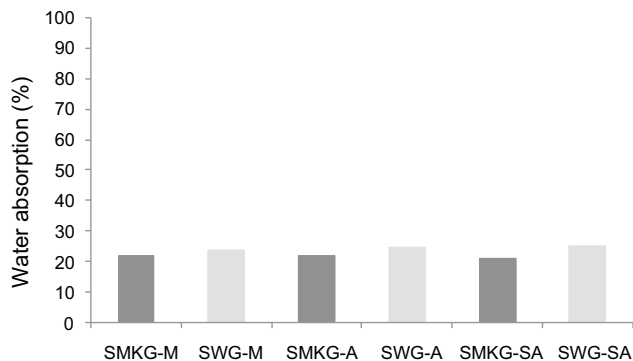


Fig. 14 – Water absorption of hardened concretes (-M: Menchar; -A: Attaf and -SA: Sidi Aich).

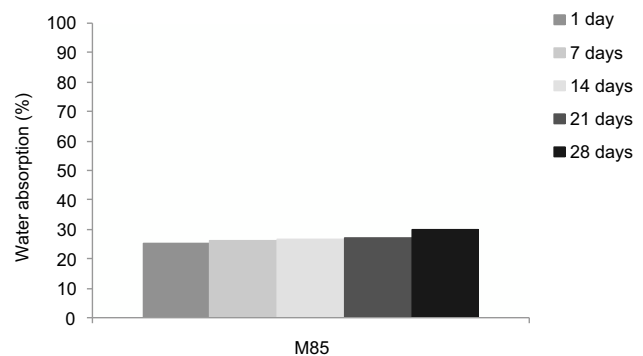


Fig. 15 – Water absorption of consolidated concrete M85 based concretes at different curing time (1; 7; 14; 21 and 28 days).

Even if this change is very slight, it indicates that polymerization process is progressing in function of curing time. At 28 days, all sand-based geopolymer concretes M85, A85 and SA85 presented practically the same relatively low mechanical resistance (around 3 MPa) (Fig. 18). For different sand/metakaolin ratios (with geopolymer matrix), the higher strength values were observed in M75, A75 and SA75 during all curing times (3.5, 3.4 and 3 MPa, respectively at 28 days; Fig. 19). It is obvious that combination of silica sand and metakaolin in ratio 75:25 gives optimal mixture to produce top strength geopolymer consolidated concrete product (Fig. 19). SEM micrographs (Fig. 20) illustrate that this ratio present the

more compact structure with more uniformly departed amorphous matrix.

On other hand, the overall low resistance values of manufactured geopolymer consolidated concrete, when compared to calcium sulphate-based ones, should be due to the low-reactive chemical character of crystallin silica sand. Moreover, low amounts of added NaOH and sodium silicate could lead to ineffective/uncomplete the polycondensation phenomenon (Fig. 18) and therefore minor compressive strength [34–36].

The evolution of water absorption values (SH-M, SMK-M, SHMK-M) for individual sets of hardened concretes is opposite to the evolution of compressive strength (SH-M, SMK-M,

Table 3 – Water absorption, open porosity and bulk density of consolidated concretes and geopolymers.

	SHMK-M	SHW-M	SMKG-M	SWG-M
Water absorption (wt.%)	48.8	54.6	22.1	23.7
Open porosity (vol.%)	51.4	56.1	24.8	26.4
Bulk density (g cm ⁻³)	1.05	1.02	1.12	1.11

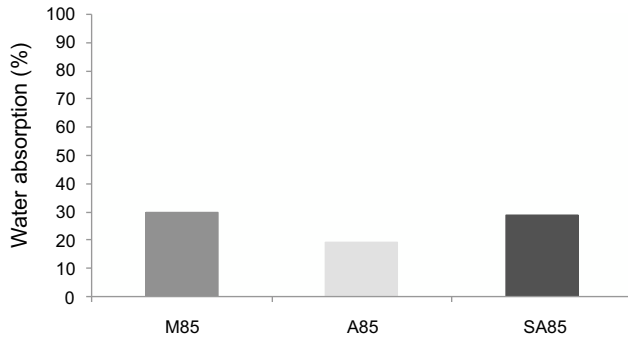


Fig. 16 – Water absorption of different consolidated concrete curing at 28 days.

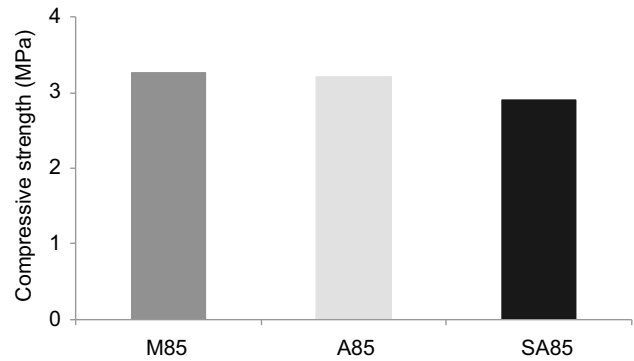


Fig. 18 – Compressive strength of consolidated concrete M85; A85 and SA85 at curing of 28 days.

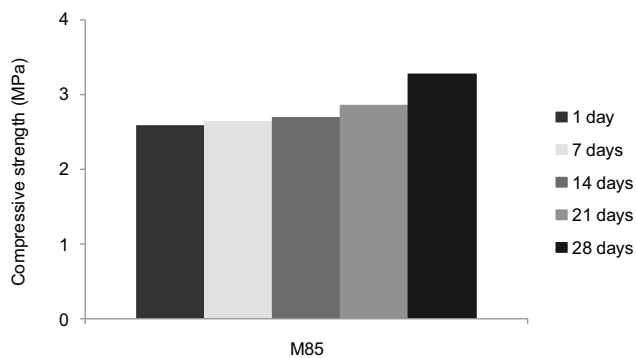


Fig. 17 – Compressive strength of consolidated concrete M85 at different curing time (1, 7, 14, 21 and 28 days).

SHMK-M). These important values of water absorption indicate that this product contains pores with larger diameters and this phenomenon is also responsible for low mechanical strength of these consolidated concrete as the fast rupture during compression is favourable in case of porous materials.

The lower results of water absorption for the geopolymer-based matrix is due to geopolymer binder which agglomerates between grains and reduce the porosity.

In summary, the obtained results show that the reactivity of calcium sulphate, metakaolin and the alkaline solution has crucial effects on the geopolymer formation and the working properties of the final materials.

Conclusions

This work has been undertaken to valorize the silica sands deposits of the Jebel Menchar (Tunisian dorsal) and the Jebels Sidi Aich and Attaf (Central Atlas) in the manufacturing of consolidated concrete. The new consolidated concrete formulations were designed by sodium silicate/NaOH activation of mixtures of metakaolin, calcium sulphate, demolition materials and three Tunisian silica sands.

The calcium sulphate-based concrete illustrated good technological properties with a compressive strength close to 15 MPa and 40–56% water adsorption. When, metakaolin and demolition reject were added the mechanical resistance

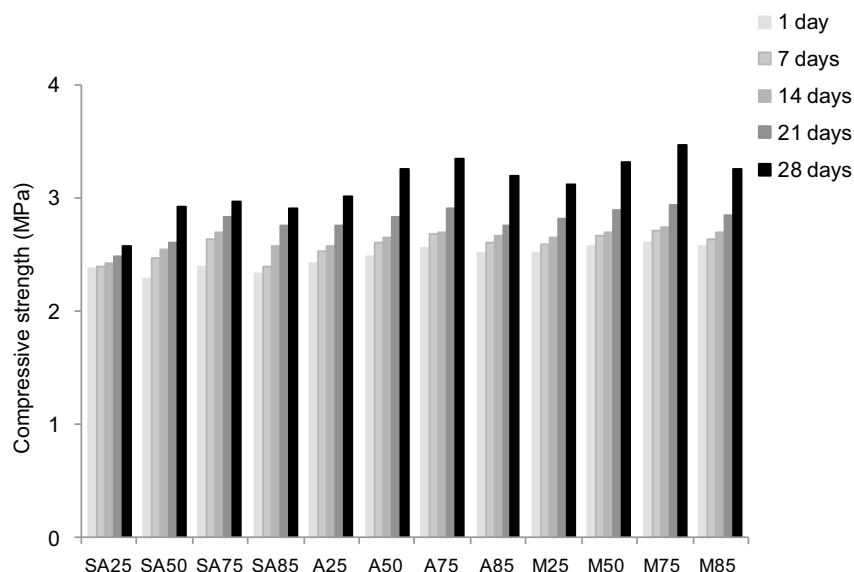


Fig. 19 – Compressive strength of consolidated concrete at different curing time (1, 7, 14, 21 and 28 days).

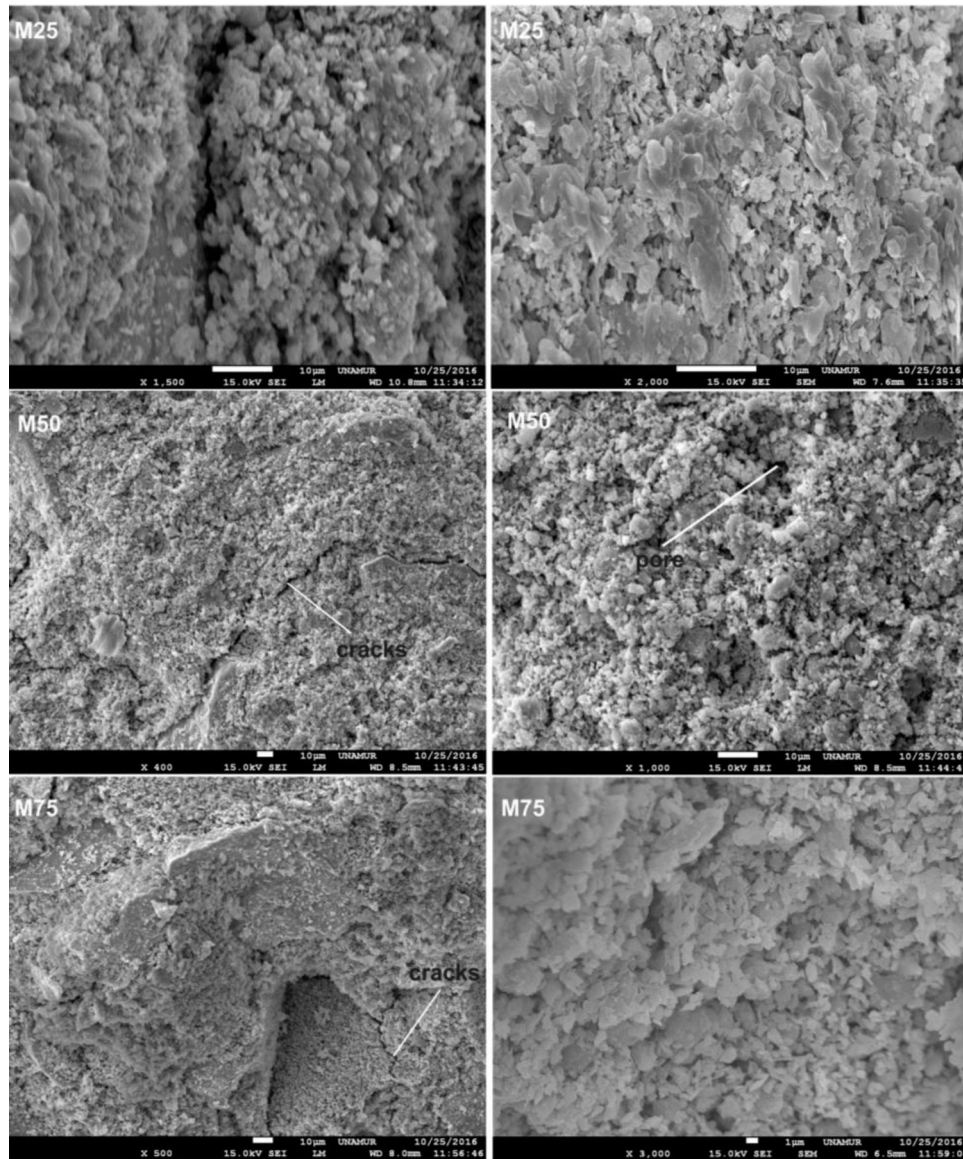


Fig. 20 – SEM micrographs of consolidated concrete.

decreased due to the lower pozzolanic properties of these materials.

Concerning the geopolymer-based sand concrete, lower compressive strength values were registered. Moreover, by replacing metakaolin (MK) by demolition materials (W), the mechanical resistance decreased by approximately 25% in all consolidated products. This behaviour should be connected to lower reactivity of the construction wastes when added to the sodium solution.

In function of curing time, that compressive strength values show an increasing trend from 1 until 28 days for geopolymer consolidated concrete. Even if the variation is very slight, it indicates that polymerization process is progressing in function of curing time. For different sand/metakaolin ratios (with geopolymer matrix), the higher strength values were observed in M75, A75 and SA75 (75% of sand) during all curing times.

All samples of the consolidated exhibit high values of water absorption than those geopolymer consolidated concrete. This

is due to consolidated concrete binder which agglomerates between grains and provides for the formation of pores.

Acknowledgements

This work was supported by FCT grant SFRH/BPD/72398/2010 and by UID/GEO/04035/2013 project. This study was supported by funding from MEDYNA: “FP7-Marie Curie Action funded under Grant Agreement PIRSES-GA- 2013-612572”, and the Tunisian Belgium Wallonie-Bruxelles International WBI Research Project “Valorisation des Argiles tunisiennes”.

REFERENCES

- [1] C. Kuenzel, L. Li, L. Vandeperre, A.R. Boccaccini, C.R. Cheeseman, Influence of sand on the mechanical properties

- of metakaolin geopolymers, *Construct. Build. Mater.* 66 (2014) 442–446, <http://dx.doi.org/10.1016/j.conbuildmat.2014.05.058>.
- [2] E. Gartner, Industrially interesting approaches to “low-CO₂” cements, *Cem. Concr. Res.* 34 (2004) 1489–1498, <http://dx.doi.org/10.1016/j.cemconres.2004.01.021>.
- [3] L.E. Burris, J.T. Ley, N. Berke, R.D. Moser, K.E. Kurtis, Novel Alternative Cementitious Materials for Development of the Next Generation of Sustainable Transportation Infrastructure, 2015, <https://www.fhwa.dot.gov/publications/research/ear/16017/index.cfm>.
- [4] M.L. Pace, A. Telesca, M. Marroccoli, G.L. Valenti, Use of industrial byproducts as alumina sources for the synthesis of calcium sulfoaluminate cements, *Environ. Sci. Technol.* 45 (2011) 6124–6128, <http://dx.doi.org/10.1021/es2005144>.
- [5] C.W. Hargis, B. Lothenbach, C.J. Müller, F. Winnefeld, Carbonation of calcium sulfoaluminate mortars, *Cem. Concr. Compos.* 80 (2017) 123–134, <http://dx.doi.org/10.1016/j.cemconcomp.2017.03.003>.
- [6] R.A. Robayo-Salazar, J. Mejia, R. Mejia de Gutierrez, Eco-efficient alkali-activated cement based on red clay brick wastes suitable for the manufacturing of building materials, *J. Clean. Prod.* 166 (2017) 242–252, <http://dx.doi.org/10.1016/j.jclepro.2017.07.243>.
- [7] M. Weil, K. Dombrowski, A. Buchwald, Life-cycle analysis of geopolymers, in: J.L. Provis, J.S.J. van Deventer (Eds.), *Geopolymers: Structure, Processing Properties and Industrial Applications*, 1st ed., Woodhead Publishing Limited, Cambridge, UK, 2009, p. 16.
- [8] T.W. Cheng, J.P. Chiu, Fire-resistant geopolymer produced by granulated blast furnace slag, *Min. Eng.* 16 (2003) 205–210, [http://dx.doi.org/10.1016/S0892-6875\(03\)00008-6](http://dx.doi.org/10.1016/S0892-6875(03)00008-6).
- [9] C. Marín-López, J.L. Reyes Araiza, A. Manzano-Ramírez, J.C. Rubio Avalos, J.J. Perez-Bueno, M.S. Muñoz-Villareal, E. Ventura-Ramos, Y. Vorobiev, Synthesis and characterization of a concrete based on metakaolin geopolymer, *Inorg. Mater.* 45 (2009) 1528–1531, <http://dx.doi.org/10.1134/S0020168509120231>.
- [10] M.J.A. Mijarsha, M.A. Megat Johari, A. Zainal Arifin, Compressive strength of treated palm oil fuel ash based geopolymer mortar containing calcium hydroxide, aluminum hydroxide and silica fume as mineral additives, *Cem. Concr. Compos.* 60 (2015) 65–81, <http://dx.doi.org/10.1016/j.cemconcomp.2015.02.007>.
- [11] I. Garcia-Lodeiro, A. Palomo, A. Fernández-Jiménez, F. Pachecho-Torgal, L.A. Labrincha, C. Leonelli, A. Palomo, P. Chindaprasirt, An overview of the chemistry of alkali-activated cement-based binder, in: *Handbook of Alkali-activated Cements, Mortars and Concretes*, 2015, pp. 19.
- [12] T.C. Ling, C.S. Poon, Use of phase change materials for thermal heat storage in concrete – an overview, *Constr. Build. Mater.* 46 (2013) 55–62, <http://dx.doi.org/10.1016/j.conbuildmat.2013.04.031>.
- [13] H. Zhao, C.H. Poon, T.C. Ling, Utilizing recycled cathode ray tube funnel glass sand as river sand replacement in the high-density concrete, *J. Clean. Prod.* 51 (2013) 184–190, <http://dx.doi.org/10.1016/j.jclepro.2013.01.025>.
- [14] M. Mansour, Develop a strategic forecast of silica sand based on supply chain decomposition, *Int. J. Eng.* 9 (2015) 9–27.
- [15] G. Fathifazl, A. Abbas, A.G. Razaqpur, O.B. Isgor, B. Fournier, S. Foo, New mixture proportioning method for concrete made with coarse recycled concrete aggregate, *J. Mater. Civil Eng.* 21 (2009) 601–611, [http://dx.doi.org/10.1061/\(ASCE\)0899-1561\(2009\)21:10\(601\)](http://dx.doi.org/10.1061/(ASCE)0899-1561(2009)21:10(601)).
- [16] N.D. Oikonomou, Recycled concrete aggregates, *Cem. Concr. Compos.* 27 (2005) 315–318, <http://dx.doi.org/10.1016/j.cemconcomp.2004.02.020>.
- [17] M.S. Juan, P.A. Gutiérrez, Study on the influence of attached mortar content on the properties of recycled concrete aggregate, *Construct. Build. Mater.* 23 (2009) 872–877, <http://dx.doi.org/10.1016/j.conbuildmat.2008.04.012>.
- [18] L. Mejri, *Tectonique Quaternaire, paléosismicité et sources sismogéniques en Tunisie Nord-Orientale: étude de la faille d’Utique* (Thèse de doctorat.), Univ Toulouse, France, 2012, pp. 167.
- [19] H. Mouakhar, A. Belkahla, H. Gabtni, T. Cavailles, J. Verges, Structural framework and basin architecture using gravity modelling in Fkirine and Djebibina area, Fkirine Exploration Block, Northern Tunisia, in: *The 13th Tunisian Petroleum Exploration and Production Conference*, 2015.
- [20] A. Said, *Tectonique active de l’Atlas Sud Tunisien: Approche structurale et morphotectonique* (Thèse de Doctorat.), Univ Toulouse III – Paul Sabatier, France, 2011, pp. 179.
- [21] M.H. Negra, H.B. Mardassi, S. Melki, Diagenetic processes and resulting variations in reservoir petrophysical characteristics within late cretaceous–early eocene carbonates in Tunisia, in: *27th I.A.S. Meeting, Alghero, Italy, 2009*, p. 624.
- [22] W. Hajjaji, K. Jeridi, P. Seabra, F. Rocha, J.A. Labrincha, F. Jamoussi, Composition and properties of glass obtained from Early Cretaceous Sidi Aich sands (central Tunisia), *Ceram. Int.* 35 (2009) 3229–3234, <http://dx.doi.org/10.1016/j.ceramint.2009.05.027>.
- [23] W. Gallala, *Les sables quartzo-feldspathiques de la Tunisie Centro-méridionale: Sédimentologie, Minéralogie, Mineralurgie et applications industrielles* (Thèse de doctorat.), Fac. Sc. Sfax, Tunisia, 2010, pp. 218.
- [24] M. Gharbi, *Interactions entre le front sud-atlasique et la marge est-tunisienne (chott – Golfe de Gabès): analyse tectono-sédimentaire, cinématique de failles et coupe équilibrée* (Thèse de doctorat.), Fac. Sc. Sfax, Tunisia, 2013, pp. 141.
- [25] W. Hajjaji, S. Andrejkovicová, C. Zanelli, M. Alshaaer, M. Dondi, J.A. Labrincha, F. Rocha, Composition and technological properties of geopolymers based on metakaolin and red mud, *Mater. Des.* 52 (2013) 648–654, <http://dx.doi.org/10.1016/j.matdes.2013.05.058>.
- [26] M. Izquierdo, X. Querol, J. Davidovits, D. Antenucci, H. Nugteren, C. Fernandez, C. Pereira, Coal fly ash-slag-based geopolymers: microstructure and metal leaching, *J. Hazard. Mater.* 166 (2009) 561–566, <http://dx.doi.org/10.1016/j.jhazmat.2008.11.063>.
- [27] W. Hajjaji, *Valorisation des sables siliceux et des argiles du cretace inferieur de la tunisie centrale et meridionale* (Thèse de doctorat.), Fac. Sc. Bizerte, Tunisia, 2011, pp. 120.
- [28] R.I. Yousef, B. El-Eswed, M. Alshaaer, F. Khalili, H. Houry, The influence of using Jordanian natural zeolite on the adsorption, physical, and mechanical properties of geopolymers products, *J. Hazard. Mater.* 165 (2008) 379–387, <http://dx.doi.org/10.1016/j.jhazmat.2008.10.004>.
- [29] W. Gallala, M.E. Gaied, M. Montacer, Detrital mode, mineralogy and geochemistry of the Sidi Aïch Formation (early cretaceous) in central and south western Tunisia: implications for provenance, tectonic setting and paleoenvironment, *J. Afr. Earth Sci.* 53 (2009) 159–170, <http://dx.doi.org/10.1016/j.jafrearsci.2009.01.002>.
- [30] T. Aloui, P. Dasgupt, F. Chaabani, Facies pattern of the Sidi Aïch formation: reconstruction of Barremian paleogeography of Central North Africa, *J. African Earth Sci.* 71 (2012) 18–42, <http://dx.doi.org/10.1016/j.jafrearsci.2012.06.004>.
- [31] S. Selmani, A. Sdiri, S. Bouaziz, E. Joussein, S. Rossignol, Effects of metakaolin addition on geopolymer prepared from natural kaolinitic clay, *Appl. Clay Sci.* 146 (2017) 457–467, <http://dx.doi.org/10.1016/j.clay.2017.06.019>.

- [32] V.F.F. Barbosa, K.J.D. Mackenzie, C. Thaumaturgo, Synthesis and characterization of materials based on inorganic polymers of alumina and silica: polysialate polymers, *Int. J. Inorg. Mater.* 2 (2000) 309–317, [http://dx.doi.org/10.1016/S1466-6049\(00\)00041-6](http://dx.doi.org/10.1016/S1466-6049(00)00041-6).
- [33] J. Wang, C. Zhang, X. Chi, Q. Jing Peng, Z. Ye, M.H. Hui, The effect of alkali on compressive of metakaolin based geopolymeric cement, *Adv. Mater. Res.* 554 (2012) 327–330, <http://dx.doi.org/10.4028/www.scientific.net/AMR.554-556.327>.
- [34] E.I. Diaz, E.N. Allouche, S. Eklund, Factors affecting the suitability of fly ash as source material for geopolymers, *J. Fuel* 89 (2010) 992–996, <http://dx.doi.org/10.1016/j.fuel.2009.09.012>.
- [35] H. Tchakoute Kouamo, *Elaboration et caractérisation de ciments géopolymères à base de scories volcaniques* (Thèse de doctorat de spécialité Physico-chimie des Matériaux Minéraux), Université Yaounde I, Cameroun, 2013, pp. 117.
- [36] A. Favier, *Mécanisme de prise et rhéologie de liants géopolymères modèles* (Thèse de doctorat de spécialité Sciences des Matériaux), Université Paris-Est, France, 2014, pp. 231.